DOI: 10.1002/cmdc.200600119

Arylthiopyrrole (AThP) Derivatives as Non-Nucleoside HIV-1 Reverse Transcriptase Inhibitors: Synthesis, Structure–Activity Relationships, and Docking Studies (Part 1)

Roberto Di Santo,*[a] Roberta Costi,[a] Marino Artico,[a] Gaetano Miele,[a] Antonio Lavecchia,[b] Ettore Novellino,[b] Alberto Bergamini,[c] Reynel Cancio,[d] and Giovanni Maga[d]

*Novel arylthio isopropyl pyridinylmethylpyrrolemethanol (AThP) derivatives **3**–**5**, which are related to capravirine (S-1153), were synthesized and tested for their ability to block the replication cycle of HIV-1 in infected cells. The newly synthesized AThPs are active in the concentration range of 0.008–53 μM. Even if compounds **3**–**5** are generally less potent than S-1153, their SI values are in some cases similar to that of the reference drug. In fact, the cytotoxicities of AThPs are generally lower than that of S-1153. Compound **4e** was the most active derivative of this series in cell-based assays; its potency is similar to that of S-1153 (EC_{50} = 8 and 3 nM, respectively), as is its selectivity index (SI = 6250 and 7000, respectively). AThP derivatives were proven to target HIV-1 RT. In fact, compounds **3**–**5** generally inhibited the viral enzyme at concentrations similar to those observed in cell-based assays. A selected number of AThPs (**4k** and **5a**,**e**) were tested against clinically relevant drug-resistant forms of recombinant reverse transcriptase (rRT) carrying the K103N and Y181I mutations. Carbamate **5e** showed an approximate 240-fold decrease in activity against Y181I, but only a 10-fold loss in potency against the K103N rRT form. Docking calculations were also performed to investigate the binding mode of compounds **2**, **4e**, **4j**, **4k** and **5e** into the non-nucleoside binding site of HIV-1 RT and to rationalize some structure–activity relationships and resistance data.*

Introduction

Highly active antiretroviral therapy (HAART) combination regimens have dramatically decreased the morbidity and mortality among patients with human immunodeficiency virus (HIV) infections.[1] However, despite the considerable success of HAART, the rapid emergence of drug-resistant HIV strains and severe side effects limit the efficacy of this therapy.[2] HAART regimens typically consist of two nucleoside reverse transcriptase inhibitors (NRTIs) and either a protease inhibitor (PI) or a non-nucleoside reverse transcriptase inhibitor (NNRTI) as a third agent, or three NRTIs. The NNRTIs have the advantage of being less toxic than NRTIs; however, there are significant problems with the development of NNRTI resistance. NNRTIs bind in a noncompetitive manner to a unique site on the enzyme, altering its ability to function. This gives highly selective suppression of HIV-1 replication with little cytotoxicity.[3] X-ray crystallography of various NNRTI–RT complexes led to the conclusion that the NNRTIs, despite their structural diversity, adopt a very similar conformational "butterfly-like" shape and appear to function through π–π interactions with aromatic side chain residues that surround the binding pocket[4] adjacent to the active site of the enzyme.[5]

Beside the rapid emergence of HIV strains resistant to current drugs and the severe side effects related to both short- and long-term treatments, the knowledge that HIV cannot be eradicated from the infected body by existing therapies[6,7] highlights the need for new drugs that are less toxic and active against the drug-resistant mutants.

Currently, only three approved drugs belong to the NNRTI class: nevirapine,[8] delavirdine,[9] and efavirenz (Figure 1).[10] In spite of this, over the last decade much effort was devoted to

[a] *Prof. Dr. R. Di Santo, Prof. Dr. R. Costi, Prof. Dr. M. Artico, Dr. G. Miele*
Istituto Pasteur–Fondazione Cenci Bolognetti
Dipartimento di Studi Farmaceutici
Università degli Studi di Roma "La Sapienza"
P.le A. Moro 5, 00185 Roma (Italy)
Fax: (+39) 6-49913150
E-mail: roberto.disanto@uniroma1.it

[b] *Prof. Dr. A. Lavecchia, Prof. Dr. E. Novellino*
Dipartimento di Chimica Farmaceutica e Tossicologica
Università degli Studi di Napoli "Federico II"
Via D. Montesanto 49, 80131 Napoli (Italy)

[c] *Prof. Dr. A. Bergamini*
Dipartimento di Sanità Pubblica e Biologia Cellulare (DSP&BC)
Università degli Studi di Roma "Tor Vergata"
Via Tor Vergata 135, 00133 Roma (Italy)

[d] *Dr. R. Cancio, Dr. G. Maga*
Istituto di Genetica Molecolare IGM–CNR
Via Abbiategrasso 207, 27100 Pavia (Italy)

Supporting information for this article is available on the WWW under http://www.chemmedchem.org or from the author.

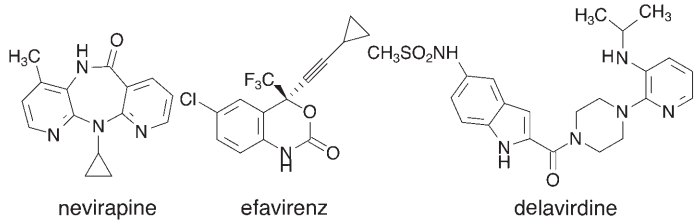

Figure 1. Structures of NNRTIs used in clinical practice.

the research of new NNRTIs as more potent and less toxic ingredients of the drug combination schemes.[11,12] Among them, capravirine (S-1153, AG1549, Figure 2),[13] a 1,2,4,5-tetrasubstituted imidazole derivative, was recently reported by the Shionogi company to inhibit HIV-1 strains that are resistant to other NNRTIs. Notably, S-1153 binds the active site of RT by an extensive network of hydrogen bonds involving the main chain of residues Lys 101, Lys 103, and Pro 236 of the p66 RT subunit. Side chain mutations are not likely to disrupt these interactions.[14] In spite of these interesting properties, S-1153 was found highly cytotoxic against MT-4 cells in in vitro assays ($CC_{50} = 24\ \mu M$). Moreover, the synthetic pathway to produce S-1153 is too cumbersome and unsuitable to generate a large number of congeners.[15]

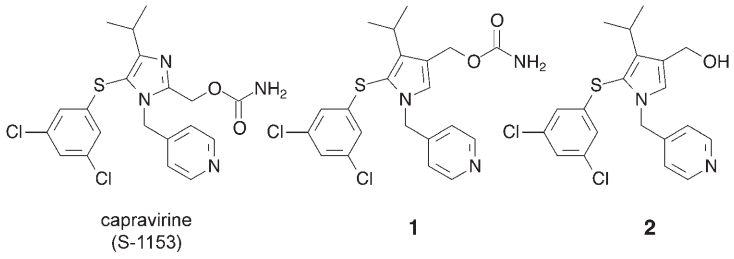

Figure 2. Capravirine (S-1153) and lead compounds **1** and **2**, which belong to the AThP class.

We recently studied a new series of analogues of S-1153, named arylthiopyrrole derivatives (AThPs), in which the imidazole ring is replaced by a pyrrole moiety.[16] A simple synthetic pathway was reported to obtain AThPs which easily allows the synthesis of a large number of congeners. The compounds 5-(3,5-dichlorophenylthio)-4-isopropyl-1-(4-pyridinylmethyl)-1*H*-pyrrol-3-ylmethyl carbamate (**1**) and 5-(3,5-dichlorophenylthio)-4-isopropyl-1-(4-pyridinylmethyl)-1*H*-pyrrole-3-methanol (**2**) were identified as leads that show potent anti-HIV-1 activity (Figure 2). Although less active than the S-1153, carbinol **2** was less cytotoxic than the reference compound, thus leading to similar selectivity indexes (> 6666 versus 7000).[16]

Herein we report extensive SAR studies of this novel class of NNRTIs. In particular, we studied the effect of substitutions on the arylthio moiety and modifications of the pyridinylmethyl group (in positions 5 and 1 of the pyrrole ring, respectively) toward anti-HIV-1 activity. Carbamate and alcohol derivatives at position 3 of the azole moiety were investigated, as well as the corresponding ester intermediates (Figure 3). Herein we describe the synthesis, cytotoxicity, and anti-HIV-1 activities of the new AThP derivatives **3**–**5** (Figure 4), as well as enzyme assays of selected derivatives against some mutated forms of recombinant reverse transcriptase (rRT) of clinical interest. Moreover, docking studies were performed to elucidate the binding mode of this novel series of AThPs in the non-nucleoside binding site (NNBS) of HIV-1 RT. In particular, we constructed models of compounds **2**, **4e**, **4j**, **4k**, and **5e** in complex with HIV-1 RT, allowing some rationalization of both structure–activity relationship (SAR) data and the effects of resistance mutations on the binding potencies of these inhibitors.

Chemistry

The synthesis of compounds **3**–**5** is depicted in Schemes 1–3. The crucial step of this synthetic pathway is an electrophilic substitution at reflux in aqueous ethanol (50%) performed on ethyl-4-isopropyl-pyrrole-3-carboxylate **6**[16] with the proper arylsulfenyl iodide as the electrophile generated in situ with the appropriate arylthiophenol, potassium iodide, and iodine. This substitution was regiospecific, leading exclusively to 5-arylthio isomers **7a**–**h** (for **7h**, see reference [17]; Scheme 1). Alkylation of pyrroles **7** with 2-, 3-, or 4-pyridylmethyl chloride hydrochloride, using tetrabutylammonium hydrogen sulfate (TBAHS) as a

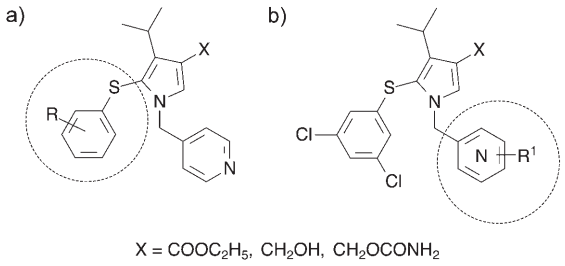

Figure 3. Planned modifications of the AThP structure: esters, carbinols, and carbamate functions at position 3 of the pyrrole ring were considered as basic structures: a) substitution on the arylthio moiety; b) modifications on the arylmethyl portion.

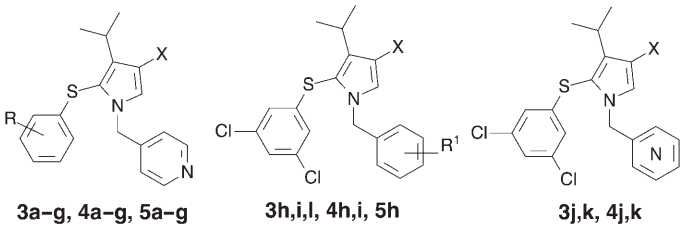

Figure 4. Novel synthesized AThP derivatives with modifications at positions 1 and 5 of the pyrrole ring.

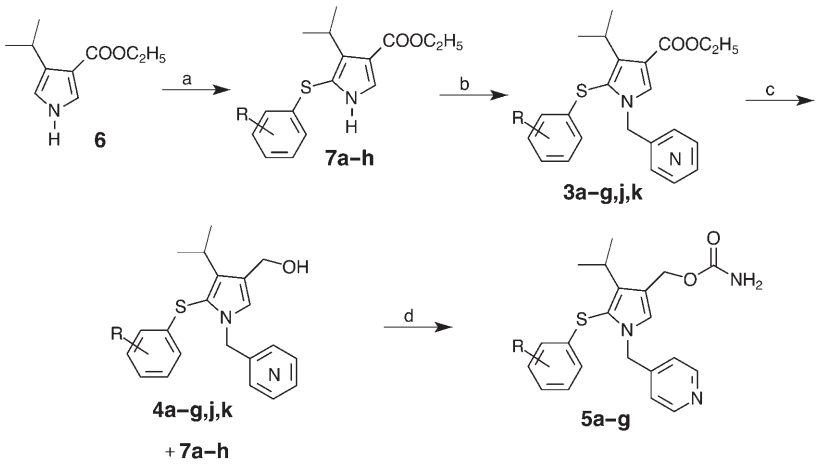

Scheme 1. Synthesis of compounds **3a–g,j,k**, **4a–g,j,k**, and **5a–g**: a) arylthiophenol, KI, I_2, EtOH/H_2O, reflux; b) pyridinylmethyl chloride hydrochloride, TBAHS, NaOH (50%), CH_2Cl_2, RT; c) $LiAlH_4$, THF, RT; d) trichloroacetylisocyanate, CH_2Cl_2, RT, 1.5 h; K_2CO_3, MeOH/H_2O, RT, 3.5 h.

phase-transfer catalyst, gave *N*-alkylpyrroles **3a–g,j,k**, which were reduced with lithium aluminum hydride to the corresponding methanols **4a–g,j,k** with partial cleavage of the *N*-alkyl substituents and consequential recovery of esters **7a–h**. The following carbamoylation was carried out in two steps by treating the alcohols **4a–g** with trichloroacetylisocyanate and hydrolyzing the trichloroacetylcarbamate intermediate in alkaline medium (potassium carbonate) to give the N-unsubstituted carbamates **5a–g** (Scheme 1).

A similar pathway, shown in Scheme 2, led to nitrobenzyl and aminobenzyl derivatives **4h,i** and **5h**. In fact, the alkylation of pyrrole **7h**[16] performed with 4-nitrobenzyl chloride and potassium carbonate as a catalyst led to ester **3i**. Reduction of the last compound with lithium aluminum hydride gave the corresponding alcohol **4i** in very poor yield, with small amounts of carbinol **8** and recovery of ester **7h**.[16] Hydrogenation of nitro derivative **3i** gave the amine **3h**, which was then converted into the methanol derivative **4h** by lithium aluminum hydride reduction. Compound **4h** was then carbamoylated with trichloroacetylisocyanate, as depicted above, to furnish **5h** (Scheme 2).

2,6-Difluorobenzyl derivative **3l** was synthesized as shown in Scheme 3. Ethyl 4-isopropyl-5-phenylthiopyrrole-3-carboxylate **9**[16] was alkylated with 2,6-difluorobenzyl bromide by using a TBAHS/sodium hydroxide system to furnish ester **3l**. The following reduction of the latter compound with lithium aluminum hydride led to the unstable carbinol **10** (Scheme 3).

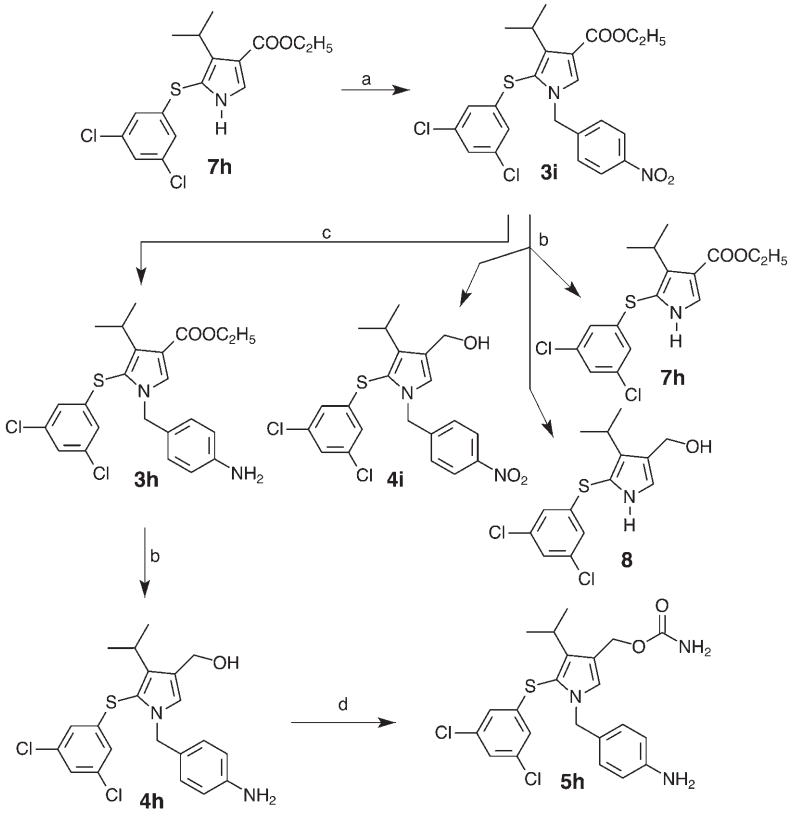

Scheme 2. Synthesis of compounds **3h,i**, **4h,i**, and **5h**: a) 4-nitrobenzyl chloride, K_2CO_3, DMF, RT, 1 h; b) $LiAlH_4$, THF, RT, 3 h; c) H_2 (207 kPa), Pd/C, EtOAc, RT, 4 h; d) trichloroacetylisocyanate, CH_2Cl_2, RT, 1.5 h; K_2CO_3, MeOH/H_2O, RT, 3.5 h.

Results and Discussion

Anti-HIV-1 cell-based assays and anti-rRT assays

The newly synthesized AThP derivatives **3**–**5** were evaluated for their cytotoxicity and anti-HIV-1 activity in MT-4 cells in comparison with nevirapine,[17] S-1153,[13] and compounds **1**[16] and **2**,[16] which were used as reference drugs. The results, expressed as CC_{50} (50% cytotoxic concentration), EC_{50} (50% HIV-1 replication inhibitory concentration) and SI (selectivity index given by the CC_{50}/EC_{50} ratio) values are summarized in Table 1. The majority of the tested AThP derivatives were found to be active in the range of 0.008–53 μM. In particular, 14 compounds showed anti-HIV-1 activities at sub-micromolar concentrations. Interestingly, the cytotoxicity of AThPs was generally low, in particular relative to that of S-1153. Owing to the above reasons, even if compounds **3**–**5** are generally less potent than S-1153, their SIs were in some cases similar to that of the reference drug. Compound **4e** was the most active derivative of this series. It was about 30-fold more potent than nevirapine and similar to S-1153 (EC_{50} = 8 and 3 nM, SI = 6250 and 7000, respectively).

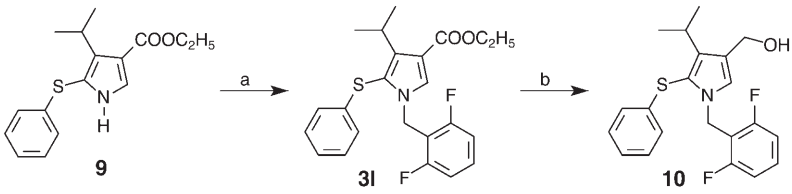

Scheme 3. Synthesis of compound **3l**: a) 2,6-difluorobenzyl bromide, TBAHS, NaOH (50%), CH_2Cl_2, RT, 3 h; b) $LiAlH_4$, THF, RT, 2 h; c) thiophenol, KI, I_2, $EtOH/H_2O$, reflux, 3 h.

Generally, the activities of carbamates **5a–h** were similar to those of alcohols **4a–k** and higher than those of the corresponding esters **3a–l**. In particular, carbamates **5c,f–h** were more potent than alcohols **4c,f–h**; in the opposite trend, alcohols **4a,b,d,e** showed EC_{50} values lower than those of the related carbamates **5a,b,d,e**.

Introduction of halogens on the arylthio moiety at position 5 of the pyrrole ring improved antiviral potency, whereas their replacement with methyl groups led to less potent derivatives in both the carbamate and alcohol series (compare **4a,b,c** with **4d,f,g**, and **5a,b,c** with **5d,f**); the exceptions to this are compounds **4e**, **5e**, and **5g**. The relevance of the position of the methyl group on the phenylthio moiety was studied. *Meta* de-

Table 1. Cytotoxicity, anti-HIV-1, and anti-rRT activities of AThP derivatives **3–5**.[a]

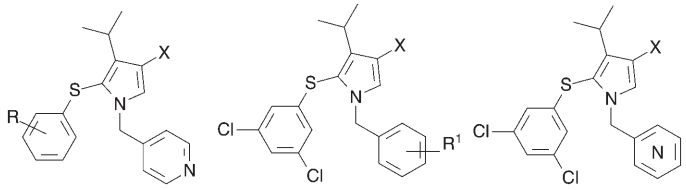

Compd	X	R	R^1	CC_{50} [μM][b]	EC_{50} [μM][c]	SI[d]	IC_{50} [μM][e] Wild-type	K103N	Y181I
3a	$COOC_2H_5$	3-F		40	3.2	12.5			
3b	$COOC_2H_5$	3-Cl		42	2.1	20			
3c	$COOC_2H_5$	3,5-difluoro		42	1.2	35	0.17		
3d	$COOC_2H_5$	2-CH_3		25	>25				
3e	$COOC_2H_5$	3-CH_3		70	1.2	58			
3f	$COOC_2H_5$	4-CH_3		60	>60				
3g	$COOC_2H_5$	3,5-dimethyl		≥200	10	20			
3h	$COOC_2H_5$		4-NH_2	>200	14	>14			
3i	$COOC_2H_5$		4-NO_2	>200	>200				
3j	$COOC_2H_5$		N2	≥200	>200				
3k	$COOC_2H_5$		N3	>200	>200				
3l	$COOC_2H_5$		2,6-difluoro	>200	>200				
4a	CH_2OH	3-F		71	0.05	1420	0.48		
4b	CH_2OH	3-Cl		65	0.1	650	0.45		
4c	CH_2OH	3,5-difluoro		60	0.4	150	0.63		
4d	CH_2OH	2-CH_3		>200	0.8	>250	4.02		
4e	CH_2OH	3-CH_3		50	0.008	6250	0.51		
4f	CH_2OH	4-CH_3		>200	53	>3.7			
4g	CH_2OH	3,5-dimethyl		≥200	0.5	≥400			
4h	CH_2OH		4-NH_2	>200	3	>67			
4i	CH_2OH		4-NO_2	45	0.15	300			
4j	CH_2OH		N2	120	3	40			
4k	CH_2OH		N3	50	0.3	167	0.24	20.5	23.55
5a	CH_2OCONH_2	3-F		≥200	0.2	≥1000	0.22	11.5	>50
5b	CH_2OCONH_2	3-Cl		>200	0.4	>500	0.28		
5c	CH_2OCONH_2	3,5-difluoro		>200	0.1	>2000	0.15		
5d	CH_2OCONH_2	2-CH_3		>200	5.4	>37			
5e	CH_2OCONH_2	3-CH_3		>200	0.12	>1667	0.11	1.0	26.65
5f	CH_2OCONH_2	4-CH_3		>200	42	>4.7			
5g	CH_2OCONH_2	3,5-dimethyl		>200	0.15	>1333	0.25		
5h	CH_2OCONH_2		4-NH_2	>200	0.1	2000			
1				>200	0.12	>1666	0.7		
2				>200	0.03	>6666	0.2		
nevirapine				>200	0.25	>800			
S-1153[f]				22	0.003	7000	0.45	0.001[f]	0.009[f]

[a] Data represent the mean of three separate experiments; variation among triplicate samples was <15%. [b] CC_{50}: compound concentration required to decrease the viability of mock-infected cells by 50% (MTT method). [c] EC_{50}: compound concentration required to achieve 50% protection of MT-4 cells from HIV-1-induced cytopathicity (MTT method). [d] SI: selectivity index, ratio of CC_{50}/EC_{50}. [e] IC_{50}: compound concentration required to inhibit HIV-1 rRT activity by 50%. [f] Published data refer to in vitro antiviral activity against resistant HIV strains (see reference [13]).

rivatives **4e** and **5e** were 50–100 times more potent than *ortho* isomers **4d** and **5d**, and 350–6600 times more potent than *para* counterparts **4f** and **5f**, respectively. These results prompted us to synthesize the dimethyl derivatives **3g**, **4g**, and **5g**, which have two methyl groups in the *meta* positions. A comparison between mono- and dimethyl derivatives led to the following results: carbamates **5e** and **5g** were equipotent, whereas the alcohol **4g** was 62-fold less potent than **4e**. Because the halogen derivatives are generally more potent than their alkyl counterparts, a further modification of the substituents on the arylthio portion was planned, in which the methyl groups of **3g**, **4g**, and **5g** would be replaced by two fluorine atoms to obtain **3c**, **4c**, and **5c**, respectively. However, these derivatives were only slightly more potent that their methyl counterparts.

The role of the nitrogen atom in position 4 of the pyridinylmethyl moiety of AThP derivatives was investigated with respect to the biological properties of this class of NNRTIs. The N4 atom of compounds **1** and **2** was shifted out the aromatic ring. Three novel derivatives were designed: 1) the amino derivatives **4h** and **5h**, which retain the basic nature and the hydrogen bond acceptor properties of the parent compounds and 2) the nitro derivative **4i**, which preserves the electronic properties of compound **2**. Interestingly, **4h** was 100-fold less potent than **2**, whereas **5h** showed activity similar to that of **1**. These results led us to hypothesize that the basic properties of the NH_2 group and/or its ability to accept hydrogen bonds could play a different role in the alcohol or carbamate series. Furthermore, the nitro derivative **4i** was fivefold less potent than the reference drug **2**. Therefore, in the alcohol series the relative potencies were **2** > **4i** > **4h**, leading us to hypothesize that the electronic properties of the substituent are more relevant to achieve a good interaction with the biological target than is the basic character or the hydrogen bond acceptor ability. A different conclusion should be made for the carbamate series, in which replacement of the pyridine nitrogen atom of **1** with an NH_2 group led to **5h**, which is equipotent to **1**. The relevance of the position of the pyridine nitrogen atom in the alcohol series was studied as well. The 2- and 3-pyridinylmethyl derivatives **4j** and **4k** were 100- and 10-fold less potent than **2**, thus indicating that the presence of N in position 4 of the pyridine unit is fundamental to obtain the highest biological activities.

As shown previously, AThPs target HIV-1 RT.[16] These results were confirmed by testing newly synthesized representative AThP derivatives against the rRT. All compounds inhibited the viral enzyme at concentrations similar to those active in cell-based assays. These results are expressed as IC_{50} values and are summarized in Table 1. In some cases the active concentrations against rRT are higher than those determined in antiviral assays; however, similar results were obtained for the reference drug S-1153. A selected number of AThPs (**4k** and **5a**,**e**) were tested against clinically relevant, drug-resistant RT forms carrying K103N and Y181I mutations. Carbinol **4k** was about 100-fold less potent against the mutated rRTs than against wild-type rRT. Similar results were found for carbamate **5a**. On the other hand, carbamate **5e** showed a similar decrease in activity against Y181I (about 240-fold), but only a 10-fold loss in potency against K103N mutated rRT.

Molecular modeling

To better elucidate the high HIV-1 RT inhibitory potencies of the newly synthesized compounds at a molecular level and to understand the structural basis of their mutant sensitivity, a binding-mode analysis was performed by means of docking experiments. Compounds **2**, **4e**, **4j**, **4k**, and **5e** were docked into the NNBS of the RT–S-1153 X-ray crystal structure (PDB code: 1EP4).[14] Docking was carried out by using the automated docking program GOLD 2.2, which has been successfully used to predict protein recognition and binding.[18–22] This program uses a genetic algorithm to explore the full range of ligand conformational flexibility with partial flexibility of the protein. Through the application of energy functions based on conformation and nonbonded contact information from the Cambridge Structural Database (CSD) and the Research Collaboratory for Structural Bioinformatics Protein Data Bank (RCSB-PDB), these protein–ligand conformations are ranked in order of fitness. By using such a program, the human element of deciding which conformation is the most probable binding conformation of a particular set of compounds in a given ligand is removed.

Prior to automated docking of the reported inhibitors, S-1153 itself was docked into the HIV-1 RT crystal structure as a means of testing program performance. The X-ray crystal structure of RT–S-1153 showed that two water molecules are directly involved in the formation of hydrogen bonds that bridge the ligand and the enzyme.[14] However, in our calculations it was not necessary to include these water molecules to reproduce the observed binding mode of S-1153 (see Experimental Section for details). A superposition of the most highly scored conformation of the ligand onto its crystallographic geometry yielded a rms deviation of 0.34 Å, thus revealing that GOLD was successful in reproducing the binding mode of S-1153 into HIV-1 RT. In addition, the hydrogen bonds predicted by GOLD were virtually identical to those found in the crystal structure.

Docking of **2**, **4e**, **4j**, **4k**, and **5e** into the RT NNBS revealed a very clear preference for a single binding position. In the most frequently occurring and most favorable result (GOLD fitness score = 47.89), **4e** was found to bind the NNBS in an orientation very similar to that of the co-crystallized inhibitor S-1153. For compounds **2**, **4j**, **4k**, and **5e**, GOLD predicted top scoring solutions (51.34, 52.00, 50.73, and 43.28, respectively) fitting into the enzyme NNBS similarly to that found for **4e**.

The energy-minimized **4k**–HIV-1 RT and **5e**–HIV-1 RT complexes are shown in Figure 5, where only the amino acids located within a distance of 3 Å from any atom of the bound inhibitor are displayed. Figure 6 illustrates the intermolecular interactions between the two compounds and the amino acid residues of the RT NNBS.

As illustrated in Figure 6a, the hydroxy group of **4k** makes a hydrogen bond with the main chain C=O group of Lys 101 (OH···O=C d = 1.8 Å), while the carbamate group of **5e** forms three H bonds with the enzyme backbone (Figure 6b): one in-

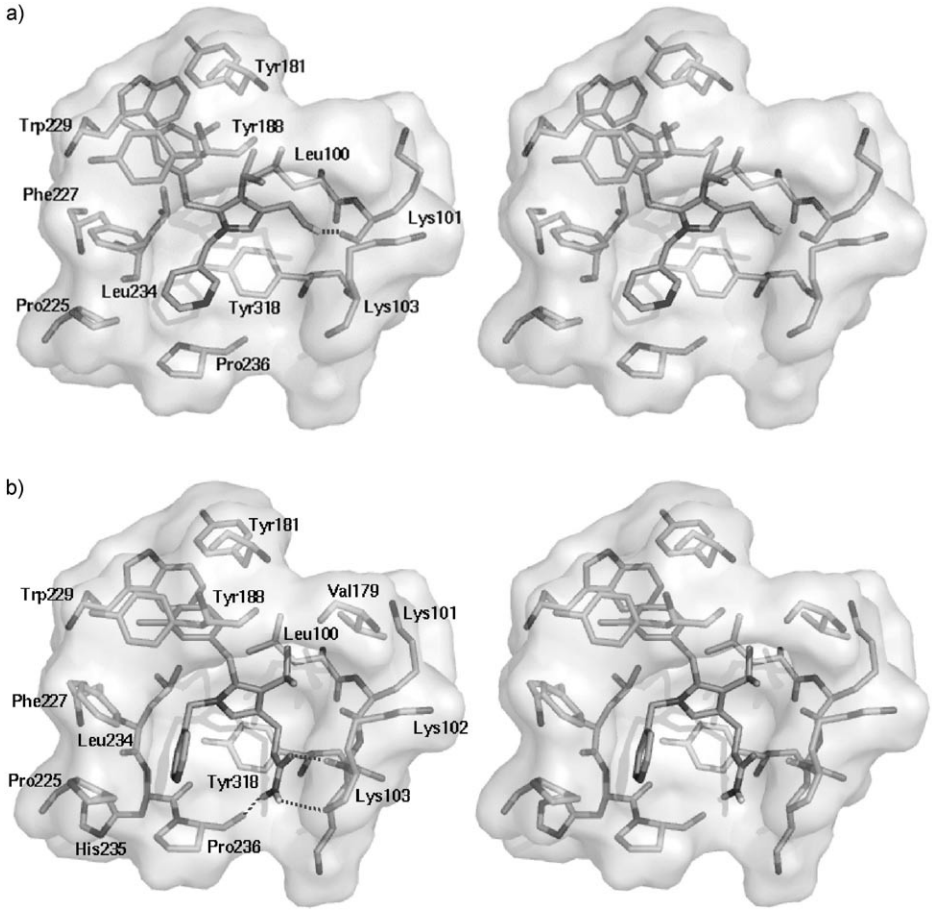

Figure 5. Stereographic views of the binding mode of compounds a) **4k** and b) **5e** in the HIV-1 RT NNBS. The protein residues located within 3 Å of any atom of the docked ligands are shown and labeled. Ligands and interacting key residues are represented as stick models, and the protein, as a transparent Connolly surface. For clarity, only interacting polar hydrogen atoms are displayed. Hydrogen bonds are shown as dashed lines.

volves the NH and main chain C=O groups of Pro 236 (NH···O=C $d = 2.0$ Å), the second occurs between the C=O oxygen atom and the main chain NH group of Lys 103 (C=O···HN $d = 1.9$ Å), and the third is engaged between the NH and main chain C=O groups of Lys 103 (NH···O=C $d = 2.4$ Å).

A hydrophobic pocket framed by the residues Gly 190, Val 179, and Val 106 was found to accommodate the isopropyl group of both ligands. The pyridinyl ring is accommodated by a large pocket mainly defined by Val 106, Pro 225, Pro 236, and Phe 227. Conducive hydrophobic interactions were found between the ring of the inhibitor and the side chains of Val 106, Pro 225, and Pro 236. In addition, the aromatic side chain of Phe 227 shows a tilted T orientation with respect to the aromatic portion of the ligand, allowing a favorable π–π interaction.

As the position of the nitrogen atom in the pyridinyl moiety of the AThP derivatives has a substantial impact on activity, we analyzed in more detail the binding modes of compounds **2**, **4k**, and **4j**, in which the pyridine nitrogen atom is located at positions 4, 3, and 2, respectively. In comparing the position of the 3-pyridinyl ring of **4k** with that of the 4-pyridinyl ring of **2** in the NNBS, we did not observe any H-bonding interaction between the pyridine N3 or N4 and the enzyme. However, a close examination of the X-ray crystal structure of the RT–S-1153 complex reveals that the pyridinyl group of S-1153 points toward the solvent region, where its N4 atom forms a hydrogen bond with a water molecule.[14] Although no solvent molecule has been taken into account in our calculations, it can be speculated that when compound **2** adapts itself to the NNBS, its 4-pyridinyl moiety would be ideally positioned to form a similar hydrogen bond with a solvent molecule. In contrast, the pyridinyl moiety of **4k** only partially exposes its N3 atom to the solvent, where it could still engage in putative H bonds with the solvent. Finally, compound **4j**, which has the nitrogen atom at position 2 of the pyridinyl moiety, does not contact any water molecule, thus preventing the possibility of hydrogen bond formation with the solvent. This is consistent with the biological data, which shows that **4k** and **4j** are less potent than **2**.

The substituted phenylthio group of the inhibitors fills the hydrophobic cleft of the NNBS made up by the aromatic rings of Tyr 181, Tyr 188, and Trp 229 as well as by Leu 100 and Leu 234. In particular, it is involved in π–π interactions with Tyr 181 and Tyr 188 and interacts with a tilted T contact with the aromatic indole nucleus of Trp 229. Such interactions are further strengthened by electron-withdrawing halogen atoms in positions 3 or 3,5 of the arylthio moiety according to the SARs discussed above. Moreover, the models of the **4k**–HIV-1 RT and **5e**–HIV-1 RT complexes show that both the 3,5-dichloro and 3-methyl substituents are responsible for an additional interaction with Trp 229, Tyr 188, and Leu 100, resulting in higher potency. Interestingly, the docking models offer an explanation of the detrimental effect of methyl groups at the *para* position on the phenyl ring: they collide with the Trp 229 indole nucleus, forcing the inhibitors in an orientation that weakens the interactions that appear to make a significant contribution to the binding energy for this series.

The drug-resistant mutation that showed the greatest effect on **5e** binding is K103N. Examination of the model of the **5e**–RT complex helps to explain these effects. K103N is the most commonly observed NNRTI-resistance mutation in the clinic, giving wide cross-resistance to most NNRTIs.[23] The resistance

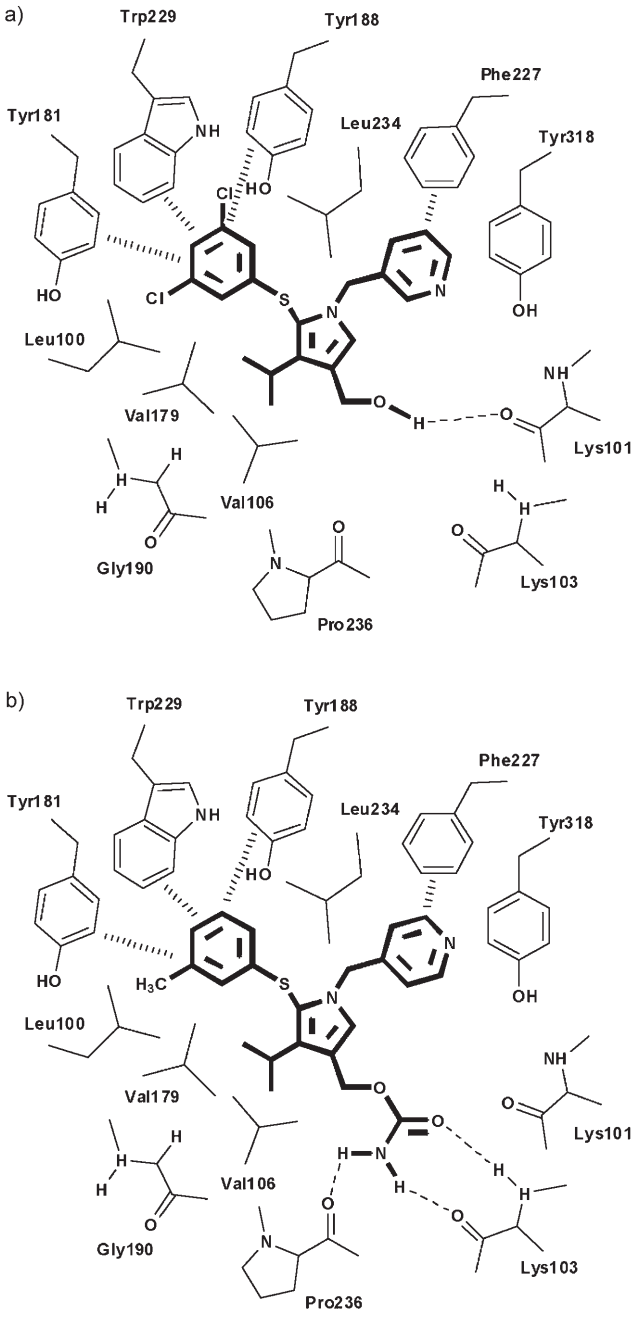

Figure 6. Possible interactions between the inhibitors a) **4k**, b) **5e**, and the surrounding residues of HIV-1 RT NNBS.

evoked by this mutation was related to stabilization of the unbound state of the enzyme by the formation of a hydrogen bond between the asparagine side chain and the OH group of Tyr188,[24] as found experimentally when the crystal structure of the K103N RT enzyme was solved. (PDB code: 1HQE).[25] However, compound **5e** shows only a 10-fold loss in potency toward the K103N mutation; differently, compound **4k** is 100-fold less potent against the mutant enzyme. Based on the present results and in the absence of a co-crystal structure with the mutant enzyme, we can speculate that resilience of **5e** to the K103N mutation could be due to the carbamate group, which is able to compete with and disrupt the hydrogen bond between Asn103 and Tyr188, in agreement with a report by Rodriguez-Barrios et al. in a recent theoretical study.[26] In contrast, the shorter CH_2OH group of compound **4k** cannot compete with and disrupt the hydrogen bond between Asn103 and Tyr188, thereby increasing the stabilization of the closed-pocket form of the mutant enzyme.

Conclusions

A series of AThP derivatives were synthesized and tested against the HIV-1 replication cycle in cell-based assays. Compound **4e** showed activity against wild-type HIV-1 (EC_{50} = 0.008 μM, CC_{50} > 200 μM, SI = 6250) similar to that of S-1153 (EC_{50} = 0.003 μM, CC_{50} = 22 μM, SI = 7000), and was about 30-fold more potent than nevirapine. AThP derivatives were proven to target HIV-1 RT in an enzyme assay. Moreover, selected derivatives were tested against clinically relevant RT mutant forms such as K103N and Y181I. Interestingly, carbamate **5e** showed only a 10-fold loss in potency against K103N mutated rRT relative to that determined against the wild-type enzyme. Docking simulations of **2**, **4e**, **4j**, **4k**, and **5e** within the NNBS of HIV-1 RT allowed the rationalization of SAR data and potencies of the compounds against the mutants.

In conclusion, AThP derivatives **4e** and **5e** are interesting NNRTIs that could be good tools to develop antiviral agents useful in clinical practice against both wild-type and mutated forms of HIV-1. On the basis of these promising anti-HIV-1 findings, the next step would be to modify the branch that makes H bonds with the NNBS and the hydrophobic alkyl group in position 4 of the AThP pyrrole ring. These experiments are described in the accompanying paper.[27]

Experimental Section

Materials: Melting points were determined on a Büchi 530 melting point apparatus and are uncorrected. IR spectra (nujol mulls) were recorded on a PerkinElmer 297 spectrophotometer. ^{1}H NMR spectra were recorded at 200 MHz on a Bruker AC 200 spectrometer using tetramethylsilane as internal reference standard. All compounds were routinely checked by TLC and ^{1}H NMR. TLC was performed with aluminum-baked silica gel plates (Fluka DC-Alufolien Kieselgel 60 F_{254}). Developed plates were visualized by UV light. Solvents were reagent grade and, when necessary, were purified and dried by standard methods. Concentration of solutions after reactions and extractions involved the use of a rotary evaporator (Büchi) operating at a reduced pressure (≈20 Torr). Organic solutions were dried over anhydrous sodium sulfate. Analytical results agreed to within ±0.40% of the theoretical values. The newly synthesized compounds **3a–l**, **4a–k**, and **5a–h** were analyzed for C, H, N, S, and, when present, Cl and F.

Syntheses: General procedure for the preparation of compounds **7a–g**; example: ethyl 5-(3-fluorophenylthio)-4-isopropyl-1*H*-pyrrole-3-carboxylate (**7a**). A solution of potassium iodide (16.9 g, 0.102 mol) and iodine (5.2 g, 0.020 mol) in aqueous ethanol (50%, 60 mL) was added dropwise to a well-stirred solution of **6**[16] (3.7 g, 0.055 mol) and 3-fluorothiophenol (6.1 g, 0.055 mol) in the same solvent (100 mL) under argon atmosphere. The mixture was held at reflux for 3.5 h, cooled, and treated with water (200 mL). The suspension that formed was extracted with ethyl acetate (3×

100 mL), and the organic extracts were collected, washed with solution of sodium thiosulfate 0.2 N (3×200 mL), then with brine (3× 200 mL), and dried. The crude product was separated on a silica gel column (chloroform as eluent) to obtain pure **7a** (2.7 g, 43%); mp: 85–86 °C (from cyclohexane); IR: $\tilde{\nu}=3250$ (NH) and 1670 cm^{-1} (CO); ^1H NMR ($CDCl_3$): $\delta=1.34$–1.45 (m, 9H, CH_3), 3.70 (m, 1H, CH), 4.35 (q, 2H, CH_2), 6.77–7.20 (m, 4H, benzene C-H), 7.62 (d, 1H, $J_{1,2}=3.3$ Hz, pyrrole C2-H), 8.50 ppm (br s, 1H, NH).

Thiophenol used as reagent; yield; reaction time; chromatographic system; melting point; recrystallization solvent; IR spectroscopic data; and ^1H NMR spectroscopic data are listed for each of the following compounds:

7b: 3-chlorothiophenol; 83%; 4 h; SiO_2 (chloroform); 90–92 °C; *n*-hexane; IR: $\tilde{\nu}=3260$ (NH) and 1675 cm^{-1} (CO); ^1H NMR ($CDCl_3$): $\delta=$ 1.33–1.43 (m, 9H, CH_3), 3.69 (m, 1H, CH), 4.33 (q, 2H, CH_2), 6.75–7.18 (m, 4H, benzene C-H), 7.60 (d, 1H, $J_{1,2}=3.3$ Hz, pyrrole C2-H), 8.47 ppm (br s, 1H, NH).

7c: 3,5-difluorothiophenol; 68%; 3 h; SiO_2 (chloroform/light petroleum ether, 1:1); 88–90 °C; cyclohexane; IR: $\tilde{\nu}=3288$ (NH) and 1673 cm^{-1} (CO); ^1H NMR ($CDCl_3$): $\delta=1.29$–1.40 (m, 9H, CH_3), 3.68 (m, 1H, CH), 4.29 (q, 2H, CH_2), 6.42–6.60 (m, 3H, benzene C-H), 7.59 (d, 1H, $J_{1,2}=3.3$ Hz, pyrrole C2-H), 8.55 ppm (br s, 1H, NH).

7d: 2-methylthiophenol; 95%; 3 h; SiO_2 (chloroform/light petroleum ether, 1:1); 94–96 °C; *n*-hexane; IR: $\tilde{\nu}=3260$ (NH) and 1670 cm^{-1} (CO); ^1H NMR ($CDCl_3$): $\delta=1.30$–1.40 (m, 9H, CH_3), 2.30 (s, 3H, $PhCH_3$), 3.66 (m, 1H, CH), 4.30 (q, 2H, CH_2), 6.75–7.15 (m, 4H, benzene C-H), 7.59 (d, 1H, $J_{1,2}=3.3$ Hz, pyrrole C2-H), 8.55 ppm (br s, 1H, NH).

7e: 3-methylthiophenol; 73%; 5.5 h; SiO_2 (chloroform); 92–95 °C; cyclohexane; IR: $\tilde{\nu}=3250$ (NH) and 1670 cm^{-1} (CO); ^1H NMR ($CDCl_3$): $\delta=1.34$–1.43 (m, 9H, CH_3), 2.30 (s, 3H, $PhCH_3$), 3.64 (m, 1H, CH), 4.32 (q, 2H, CH_2), 6.76–7.14 (m, 4H, benzene C-H), 7.57 (d, 1H, $J_{1,2}=3.3$ Hz, pyrrole C2-H), 8.45 ppm (br s, 1H, NH).

7f: 4-methylthiophenol; 38%; 2 h; SiO_2 (chloroform/light petroleum ether, 1:1); 89–91 °C; *n*-hexane; IR: $\tilde{\nu}=3240$ (NH) and 1675 cm^{-1} (CO); ^1H NMR ($CDCl_3$): $\delta=1.35$–1.45 (m, 9H, CH_3), 2.32 (s, 3H, $PhCH_3$), 3.65 (m, 1H, CH), 4.30 (q, 2H, CH_2), 6.75–7.10 (m, 4H, benzene C-H), 7.56 (d, 1H, $J_{1,2}=3.3$ Hz, pyrrole C2-H), 8.40 ppm (br s, 1H, NH).

7g: 3,5-dimethylthiophenol; 69%; 5 h; SiO_2 (chloroform); 90–92 °C; cyclohexane; IR: $\tilde{\nu}=3240$ (NH) and 1670 cm^{-1} (CO); ^1H NMR ($CDCl_3$): $\delta=1.35$–1.44 (m, 9H, CH_3), 2.26 (s, 6H, $PhCH_3$), 3.62 (m, 1H, CH), 4.33 (q, 2H, CH_2), 6.63 and 6.78 (2 s, 3H, benzene C-H), 7.57 (d, 1H, $J_{1,2}=3.3$ Hz, pyrrole C2-H), 8.34 ppm (br s, 1H, NH).

General procedure for the preparation of compounds **3a**–**g**,**j**–**l**; example: ethyl 5-(3-fluorophenylthio)-4-isopropyl-1-(4-pyridinylmethyl)-1*H*-pyrrole-3-carboxylate (**3a**). A well-cooled solution of tetrabutylammonium hydrogen sulfate (TBAHS, 2.5 g, 7.4 mmol) and 4-(chloromethyl)pyridine hydrochloride (1.2 g, 7.6 mmol) in dichloromethane (11 mL) was treated with sodium hydroxide 50% (11 mL) and with a solution of **7a** (2.3 g, 7.4 mmol) in dichloromethane (16 mL), in turn. The mixture was stirred at room temperature for 1.5 h, then water (50 mL) was added, and the suspension that formed was extracted with chloroform (3×50 mL). The organic extracts were collected, washed with brine, and dried. The evaporation of the solvent gave the crude product, which was separated on a silica gel column (ethyl acetate as eluent) to give pure **3a** (2.9 g, 100%); oil; IR: $\tilde{\nu}=1690$ cm^{-1} (CO); ^1H NMR ($CDCl_3$): $\delta=1.35$–1.43 (m, 9H, CH_3), 3.60 (m, 1H, CH), 4.31 (q, 2H, CH_2CH_3), 5.12 (s, 2H, CH_2), 6.60–7.20 (m, 6H, benzene C-H and pyridine C3-H and C5-H), 7.64 (s, 1H, pyrrole C2-H), 8.47–8.50 ppm (m, 2H, pyridine C2-H and C6-H).

Alkylating reagent; yield; reaction time; chromatographic system; melting point; recrystallization solvent; IR spectroscopic data; and ^1H NMR spectroscopic data are listed for each of the following compounds:

3b: 4-(chloromethyl)pyridine hydrochloride; 64%; 1 h; SiO_2 (ethyl acetate); oil; IR: $\tilde{\nu}=1710$ cm^{-1} (CO); ^1H NMR ($CDCl_3$): $\delta=1.32$–1.43 (m, 9H, CH_3), 3.60 (m, 1H, CH), 4.32 (q, 2H, CH_2CH_3), 5.12 (s, 2H, CH_2), 6.69–7.20 (m, 6H, benzene C-H and pyridine C3-H and C5-H), 7.64 (s, 1H, pyrrole C2-H), 8.47–8.50 ppm (m, 2H, pyridine C2-H and C6-H).

3c: 4-(chloromethyl)pyridine hydrochloride; 33%; 1.5 h; SiO_2 (chloroform/ethyl acetate, 1:9); oil; IR: $\tilde{\nu}=1718$ cm^{-1} (CO); ^1H NMR ($CDCl_3$): $\delta=1.35$–1.44 (m, 9H, CH_3), 3.60 (m, 1H, CH), 4.34 (q, 2H, CH_2CH_3), 5.12 (s, 2H, CH_2), 6.33–6.40 (m, 3H, benzene C-H), 6.91–6.94 (m, 2H, pyridine C3-H and C5-H), 7.67 (s, 1H, pyrrole C2-H), 8.50–8.53 ppm (m, 2H, pyridine C2-H and C6-H).

3d: 4-(chloromethyl)pyridine hydrochloride; 86%; 2 h; SiO_2 (chloroform/ethyl acetate, 9:1); 85–87 °C; cyclohexane; IR: $\tilde{\nu}=1715$ cm^{-1} (CO); ^1H NMR ($CDCl_3$): $\delta=1.32$–1.39 (m, 9H, CH_3), 2.35 (s, 3H, $PhCH_3$), 3.60 (m, 1H, CH), 4.29 (q, 2H, CH_2CH_3), 5.03 (s, 2H, CH_2), 6.33–6.40 (m, 1H, benzene C-H), 6.86–7.20 (m, 5H, benzene C-H, pyridine C3-H and C5-H), 7.60 (s, 1H, pyrrole C2-H), 8.44–8.47 ppm (m, 2H, pyridine C2-H and C6-H).

3e: 4-(chloromethyl)pyridine hydrochloride; 53%; 1.5 h; SiO_2 (ethyl acetate); 72–74 °C; *n*-hexane; IR: $\tilde{\nu}=1690$ cm^{-1} (CO); ^1H NMR ($CDCl_3$): $\delta=1.27$–1.46 (m, 9H, CH_3), 2.20 (s, 3H, $PhCH_3$), 3.61 (m, 1H, CH), 4.27 (q, 2H, CH_2CH_3), 5.08 (s, 2H, CH_2), 6.61–6.65 (m, 2H, benzene C-H), 6.85 (d, 2H, $J_{2,3}=5.8$ Hz, pyridine C3-H and C5-H), 6.99–7.07 (m, 2H, benzene C-H), 7.57 (s, 1H, pyrrole C2-H), 8.44 ppm (d, 2H, $J_{2,3}=5.8$ Hz, pyridine C2-H and C6-H).

3f: 4-(chloromethyl)pyridine hydrochloride; 79%; 2 h; SiO_2 (chloroform/ethyl acetate, 9:1); oil; IR: $\tilde{\nu}=1714$ cm^{-1} (CO); ^1H NMR ($CDCl_3$): $\delta=1.35$–1.42 (m, 9H, CH_3), 2.29 (s, 3H, $PhCH_3$), 3.62 (m, 1H, CH), 4.42 (q, 2H, CH_2CH_3), 5.12 (s, 2H, CH_2), 6.72–7.20 (m, 6H, benzene C-H, pyridine C3-H and C5-H), 7.58 (s, 1H, pyrrole C2-H), 8.44 ppm (d, 2H, $J_{2,3}=5.8$ Hz, pyridine C2-H and C6-H).

3g: 4-(chloromethyl)pyridine hydrochloride; 77%; 1.5 h; SiO_2 (ethyl acetate); 92–94 °C; *n*-hexane; IR: $\tilde{\nu}=1700$ cm^{-1} (CO); ^1H NMR ($CDCl_3$): $\delta=1.36$–1.43 (m, 9H, CH_3), 2.20 (s, 6H, $PhCH_3$), 3.64 (m, 1H, CH), 4.33 (q, 2H, CH_2CH_3), 5.12 (s, 2H, CH_2), 6.49 (s, 2H, benzene C2-H and C6-H), 6.72 (s, 1H, benzene C4-H), 6.89 (d, 2H, $J_{2,3}=$ 6.0 Hz, pyridine C3-H and C5-H), 7.60 (s, 1H, pyrrole C2-H), 8.48 ppm (m, 2H, $J_{2,3}=6.0$ Hz, pyridine C2-H and C6-H).

3j: 2-(chloromethyl)pyridine hydrochloride; 97%; 2 h; SiO_2 (chloroform/ethyl acetate, 1:1); 122–124 °C; cyclohexane; IR: $\tilde{\nu}=$ 1710 cm^{-1} (CO); ^1H NMR ($CDCl_3$): $\delta=1.34$–1.43 (m, 9H, CH_3), 3.21 (m, 1H, CH), 4.32 (q, 2H, CH_2CH_3), 5.25 (s, 2H, CH_2), 6.65 (d, 2H, $J_m=1.8$ Hz, benzene C2-H and C6-H), 6.77–6.80 (m, 1H, pyridine C3-H), 7.00 (t, 1H, $J_m=1.8$ Hz, benzene C4-H), 7.15–7.20 (m, 1H, pyridine C-H), 7.49–7.52 (m, 1H, pyridine CH), 7.79 (s, 1H, pyrrole C2-H), 8.49–8.51 ppm (m, 1H, pyridine C6-H).

3k: 3-(chloromethyl)pyridine hydrochloride; 82%; 2 h; SiO_2 (chloroform/ethyl acetate, 1:1); 132–134 °C; cyclohexane; IR: $\tilde{\nu}=$ 1700 cm^{-1} (CO); ^1H NMR ($CDCl_3$): $\delta=1.33$–1.44 (m, 9H, CH_3), 3.57 (m, 1H, CH), 4.34 (q, 2H, CH_2CH_3), 5.13 (s, 2H, CH_2), 6.65 (d, 2H, $J_m=1.6$ Hz, benzene C2-H and C6-H), 7.06 (t, 1H, $J_m=1.6$ Hz, ben-

zene C4-H), 7.17–7.23 (m, 1H, pyridine C5-H), 7.30–7.36 (m, 1H, pyridine C4-H), 7.67 (s, 1H, pyrrole C2-H), 8.42 (d, 1H, $J_{2,4}=1.9$ Hz, pyridine C2-H), 8.49 ppm (dd, 1H, $J_{5,6}=6.4$ Hz, $J_{4,6}=1.9$ Hz, pyridine C6-H).

3l: 2,6-difluorobenzyl bromide; 98%; 3 h; SiO_2 (chloroform/light petroleum ether, 1:1); oil; IR: $\tilde{\nu}=1690$ cm^{-1} (CO); ^{1}H NMR ($CDCl_3$): $\delta=1.26$–1.37 (m, 9H, CH_3), 3.58 (m, 1H, CH), 4.26 (q, 2H, CH_2CH_3), 5.14 (s, 2H, CH_2), 6.73–7.25 (m, 8H, benzene C-H), 7.47 ppm (s, 1H, pyrrole C2-H).

Ethyl 1-(4-aminophenylmethyl)-5-[(3,5-dichloro)phenylthio]-4-isopropyl-1*H*-pyrrole-3-carboxylate (**3h**): A solution of **3i** (1.0, 2.0 mmol) in ethyl acetate (150 mL) was hydrogenated in a Parr apparatus at room temperature with palladium on charcoal 10% (200 mg) at a starting pressure of 207 kPa. After stirring for 4 h, the catalyst was filtered off, the filtrate was dried, and the solvent was evaporated to give the crude amine, which was then separated on a silica gel column (ethyl acetate/*n*-hexane, 5:1 as eluent) to furnish pure **3h** (590 mg, 63%); mp: 107–110 °C (from cyclohexane); IR: $\tilde{\nu}=3410$, 3310 (NH_2) and 1680 cm^{-1} (CO); ^{1}H NMR ($CDCl_3$): $\delta=$ 1.32–1.47 (m, 9H, CH_3), 3.53–3.67 (m, 3H, NH_2 and CH), 4.32 (q, 2H, CH_2CH_3), 4.97 (s, 2H, CH_2), 6.54 (d, 2H, $J_o=8.3$ Hz, benzene C2-H and C6-H), 6.64 (d, 2H, $J_m=1.8$ Hz, PhS C2-H and C6-H), 6.88 (d, 2H, $J_o=8.3$ Hz, benzene C3-H and C5-H), 7.05 (t, 1H, $J_m=1.8$ Hz, PhS C4-H), 7.61 ppm (s, 1H, pyrrole C2-H).

3i: A well-stirred suspension of **7h** (1.0 g, 2.8 mmol), 4-nitrobenzyl chloride (540 mg, 3.2 mmol), and K_2CO_3 (770 mg, 5.6 mmol) in anhydrous *N*,*N*-dimethylformamide (3 mL) was heated at 90 °C for 1 hour. The reaction was treated with water (20 mL) and extracted with ethyl acetate (3×20 mL). The collected extracts were washed with brine (3×50 mL), dried, and the solvent was evaporated. The crude product was separated on a silica gel column (chloroform/light petroleum ether, 5:1 as eluent) to give pure **3i** (1.2 mg, 87%); mp: 110–112 °C (from cyclohexane); IR: $\tilde{\nu}=1690$ cm^{-1} (CO); ^{1}H NMR ($CDCl_3$): $\delta=1.34$–1.45 (m, 9H, CH_3), 3.63 (m, 1H, CH), 4.35 (q, 2H, CH_2CH_3), 5.23 (s, 2H, CH_2), 6.59 (d, 2H, $J_m=1.7$ Hz, PhS C2-H and C6-H), 7.01 (d, 1H, $J_m=1.7$ Hz, PhS C4-H), 7.17 (m, 2H, benzene C2-H and C6-H), 7.73 (s, 1H, pyrrole C2-H), 8.07 ppm (m, 2H, benzene C3-H and C5-H).

General procedure for the preparation of compounds **4a**–**i**,**j**,**k** and **10**; example: ethyl 4-isopropyl-5-(3-fluorophenylthio)-1-(4-pyridinylmethyl)-1*H*-pyrrole-3-methanol (**4a**). A solution of **3a** (2.2 g, 5.5 mmol) in anhydrous tetrahydrofuran (140 mL) was added dropwise to a well-stirred suspension of lithium aluminum hydride (1.1 g, 27.9 mmol) in the same solvent (140 mL) cooled at 0 °C. After addition, the mixture was stirred at room temperature for 18 h and then carefully treated with crushed ice. The inorganic precipitate was removed, and the solution was concentrated and treated with ethyl acetate (100 mL). The organic solution was shaken with brine (3×100 mL), dried, and evaporated to give crude product, which was separated on a silica gel column (ethyl acetate as eluent) to obtain pure **4a** (1.2 g, 62% yield); oil; IR: $\tilde{\nu}=$ 3250 cm^{-1} (OH); ^{1}H NMR ($CDCl_3$): $\delta=1.32$ (d, 6H, CH_3), 2.00 (br s, 1H, OH), 3.20 (m, 1H, CH), 4.73 (s, 2H, CH_2OH), 5.08 (s, 2H, CH_2), 6.47–7.30 (m, 7H, pyridine C3-H and C5-H, pyrrole C2-H and benzene C-H), 8.42–8.46 ppm (m, 2H, pyridine C2-H and C6-H).

Equivalents of lithium aluminum hydride; yield; reaction time; chromatographic system; melting point; recrystallization solvent; IR spectroscopic data; and ^{1}H NMR spectroscopic data are listed for each of the following compounds:

4b: 5; 51%; 18 h; SiO_2 (ethyl acetate); oil; IR: $\tilde{\nu}=3250$ cm^{-1} (OH); ^{1}H NMR ($CDCl_3$): $\delta=1.32$ (d, 6H, CH_3), 2.00 (br s, 1H, OH), 3.20 (m, 1H, CH), 4.73 (s, 2H, CH_2OH), 5.08 (s, 2H, CH_2), 6.80–7.30 (m, 7H, pyridine C3-H and C5-H, pyrrole C2-H and benzene C-H), 8.43–8.46 ppm (m, 2H, pyridine C2-H and C6-H).

4c: 7.5; 22%; 22 h; SiO_2 (ethyl acetate); 123–125 °C; benzene/cyclohexane; IR: $\tilde{\nu}=3250$ cm^{-1} (OH); ^{1}H NMR ($CDCl_3$): $\delta=1.31$ (d, 6H, CH_3), 2.05 (br s, 1H, OH), 3.21 (m, 1H, CH), 4.74 (s, 2H, CH_2OH), 5.10 (s, 2H, CH_2), 6.48–7.35 (m, 6H, pyridine C3-H and C5-H, pyrrole C2-H and benzene C-H), 8.43–8.47 ppm (m, 2H, pyridine C2-H and C6-H).

4d: 5; 46%; 3 h; SiO_2 (ethyl acetate); 148–150 °C; toluene; IR: $\tilde{\nu}=$ 3201 cm^{-1} (OH); ^{1}H NMR ($CDCl_3$): $\delta=1.32$ (d, 6H, CH_3), 1.98 (br s, 1H, OH), 2.35(s, 3H, $PhCH_3$), 3.20 (m, 1H, CH), 4.70 (s, 2H, CH_2OH), 5.00 (s, 2H, CH_2), 6,45–6.48 (m,1H, benzene C-H), 6.85–6.95 (m, 6H, pyridine C3-H and C5-H, pyrrole C2-H and benzene C-H), 8.39–8.42 ppm (m, 2H, pyridine C2-H and C6-H).

4e: 5; 28%; 22 h; SiO_2 (ethyl acetate); oil; IR: $\tilde{\nu}=3220$ cm^{-1} (OH); ^{1}H NMR ($CDCl_3$): $\delta=1.27$ (d, 6H, $CHCH_3$), 2.20 (s, 3H, CH_3), 2.56 (br s, 1H, OH), 3.26 (m, 1H, CH), 4.69 (s, 2H, CH_2OH), 5.05 (s, 2H, CH_2), 6.59–6.68 (m, 2H, benzene C-H), 6.82–7.05 (m, 5H, pyridine C3-H and C5-H, pyrrole C2-H and benzene C-H), 8.35 ppm (d, 2H, $J_{2,3}=4.5$ Hz, pyridine C2-H and C6-H).

4f: 6; 34%; 22 h; SiO_2 (ethyl acetate); 113–114 °C; benzene/*n*-hexane; IR: $\tilde{\nu}=3220$ cm^{-1} (OH); ^{1}H NMR ($CDCl_3$): $\delta=1.32$ (d, 6H, $CHCH_3$), 2.20 (br s, 1H, OH), 2.60 (s, 3H, CH_3), 3.30 (m, 1H, CH), 4.72 (s, 2H, CH_2OH), 5.07 (s, 2H, CH_2), 6.70–7.02 (m, 7H, benzene C-H, pyridine C3-H and C5-H, pyrrole C2-H), 8.41–8.44 ppm (m, 2H, pyridine C2-H and C6-H).

4g: 5; 25%; 4.5 h; SiO_2 (ethyl acetate); oil; IR:$\tilde{\nu}=3210$ cm^{-1} (OH); ^{1}H NMR ($CDCl_3$): $\delta=1.32$ (d, 6H, $CHCH_3$), 2.00 (br s, 1H, OH), 2.20 (s, 6H, CH_3), 3.20 (m, 1H, CH), 4.73 (s, 2H, CH_2OH), 5.09 (s, 2H, CH_2), 6.49 (s, 2H, benzene C2-H and C6-H), 6.70 (s, 1H, benzene C4-H), 6.90 (d, 2H, $J_{2,3}=6.0$ Hz, pyridine C3-H and C5-H), 6.96 (s, 1H, pyrrole C2-H), 8.41 ppm (d, 2H, $J_{2,3}=6.0$ Hz, pyridine C2-H and C6-H).

4h: 5; 33%; 2.5 h; SiO_2 (*n*-hexane/ethyl acetate 2:1); oil; IR: $\tilde{\nu}=$ 3300 cm^{-1} (OH and NH_2); ^{1}H NMR ($CDCl_3$): $\delta=1.30$ (d, 6H, CH_3), 1.64 (br s, 1H, OH), 3.15 (m, 1H, CH), 3.70 (br s, 2H, NH_2), 4.67 (s, 2H, CH_2OH), 4.94 (s, 2H, CH_2), 6.54 (d, 2H, $J_o=8.4$ Hz, benzene C2-H and C6-H), 6.66 (d, 2H, $J_m=1.8$ Hz, PhS C2-H and C6-H), 6.88 (d, 2H, $J_o=8.4$ Hz, benzene C3-H and C5-H), 6.96 (s, 1H, pyrrole C2-H), 7.04 ppm (t, 1H, $J_m=1.8$ Hz, PhS C4-H).

4i: 7.5; 10%; 3 h; SiO_2 (*n*-hexane/ethyl acetate 1:1); oil; IR: $\tilde{\nu}=$ 3320 cm^{-1} (OH); ^{1}H NMR ($CDCl_3$): $\delta=1.31$ (d, 6H, CH_3), 1.62 (br s, 1H, OH), 3.10 (m, 1H, CH), 4.75 (s, 2H, CH_2OH), 5.19 (s, 2H, CH_2), 6.60 (d, 2H, $J_m=1.9$ Hz, PhS C2-H and C6-H), 7.00 (t, 1H, $J_m=$ 1.9 Hz, PhS C4-H), 7.08 (s, 1H, pyrrole C2-H), 7.75 (d, 2H, $J_o=$ 8.7 Hz, benzene C2-H and C6-H), 8.07 ppm (d, 2H, 8.25 $J_o=8.7$ Hz, benzene C3-H and C5-H); the following compounds were obtained after chromatography: **7h**: 30%; **8**: 5%; oil; IR: $\tilde{\nu}=3300$ cm^{-1} (OH); ^{1}H NMR ($CDCl_3$): $\delta=1.31$ (d, 6H, CH_3), 1.67 (br s, 1H, OH), 3.20 (m, 1H, CH), 4.70 (s, 2H, CH_2OH), 6.82 (d, 2H, $J_m=2.0$ Hz, benzene C2-H and C6-H), 6.99 (d, 1H, $J_{1,2}=2.9$ Hz, pyrrole C2-H), 7.10 (t, 1H, $J_m=2.0$ Hz, benzene C4-H), 8.25 ppm (br s, 1H, NH).

4j: 5; 27%; 3.5 h; SiO_2 (ethyl acetate); oil; IR: $\tilde{\nu}=3300$ cm^{-1} (OH); ^{1}H NMR ($CDCl_3$): $\delta=1.30$ (d, 6H, CH_3), 1.71 (br s, 1H, OH), 3.22–3.26 (m, 1H, CH), 4.72 (s, 2H, CH_2OH), 5.21 (s, 2H, CH_2), 6.66 (d, 2H, $J_m=$ 1.6 Hz, benzene C2-H and C6-H), 6.80 (d, 1H, $J_{3,4}=7.8$ Hz, pyridine C3-H), 6.99 (t, 1H, $J_m=1.6$ Hz, benzene C4-H), 7.10–7.14 (m, 2H,

pyrrole C2-H and pyridine C-H), 7.49–7.52 (m, 1H, pyridine C-H), 8.50 ppm (d, 1H, $J_{5,6}=7.8$ Hz, pyridine C6-H).

4k: 5; 66%; 3.5 h; SiO_2 (ethyl acetate); 95–96 °C; cyclohexane; IR: $\tilde{\nu}=3220$ cm^{-1} (OH); ^{1}H NMR ($CDCl_3$): $\delta=1.30$ (d, 6H, CH_3), 1.85 (br s, 1H, OH), 3.30 (m, 1H, CH), 4.71 (s, 2H, CH_2OH), 5.10 (s, 2H, CH_2), 6.66 (d, 2H, $J_m=1.7$ Hz, benzene C2-H and C6-H), 7.03–7.05 (m, 2H, pyrrole C2-H and benzene C4-H), 7.14–7.20 (m, 1H, pyridine C5-H), 7.30–7.35 (m, 1H, pyridine C4-H), 8.38 (d, 1H, $J_{2,4}=1.7$ Hz, pyridine C2-H), 8.45 ppm (dd, 1H, $J_{5,6}=6.4$ Hz, $J_{2,4}=1.7$ Hz, pyridine C6-H).

10: 5; 50%; 3.5 h; SiO_2 (ethyl acetate); oil; IR: $\tilde{\nu}=3300$ cm^{-1} (OH); ^{1}H NMR ($CDCl_3$): $\delta=1.19$ (d, 6H, CH_3), 1.60 (br s, 1H, OH), 3.20 (m, 1H, CH), 4.45 (s, 2H, CH_2OH), 5.10 (s, 2H, CH_2), 6.70–7.25 ppm (m, 9H, pyrrole C2-H and benzene C-H). This compound degrades within a few hours after isolation.

General procedure for the preparation of compounds **5a–h**; example: ethyl 5-(3-fluorophenylthio)-4-isopropyl-1-(4-pyridinylmethyl)-1*H*-pyrrol-3-ylmethyl carbamate (**5a**). Trichloroacetylisocyanate (590 mg, 3.2 mmol) was added dropwise to a well-stirred solution of **4a** (950 mg, 2.7 mmol) in dichloromethane (11 mL) cooled at 0 °C. Then the mixture was stirred at room temperature for 1.5 h, and the solvent was removed under reduced pressure. The residue was dissolved in methanol (3.6 mL), and the resulting solution was cooled at 0 °C and treated with a cold solution of potassium carbonate (1.5 g, 10.6 mmol) in water (3.6 mL). The resulting suspension was stirred at room temperature for 3.5 h, then the methanol was removed under reduced pressure, and the residue was treated with ethyl acetate (200 mL). The organic solution was washed with brine (3×20 mL) and dried. Evaporation of the solvent gave the crude product, which was separated on a silica gel column (ethyl acetate as eluent) to give pure **5a** (360 mg, 34%); oil; IR: $\tilde{\nu}=3300$, 3130 (NH_2) and 1695 cm^{-1} (CO); ^{1}H NMR ($CDCl_3$): $\delta=1.31$ (d, 6H, CH_3), 3.20 (m, 1H, CH), 4.75 (br s, 2H, NH_2), 5.08 (s, 2H, CH_2OCONH$_2$), 5.13 (s, 2H, CH_2), 6.46–7.15 (m, 7H, pyridine C3-H and C5-H, pyrrole C2-H and benzene C-H), 8.45–8.49 ppm (m, 2H, pyridine C2-H and C6-H).

Yield; chromatographic system; melting point; recrystallization solvent; IR spectroscopic data; and ^{1}H NMR spectroscopic data are listed for each of the following compounds:

5b: 51%; SiO_2 (ethyl acetate); 110–112 °C; cyclohexane; IR: $\tilde{\nu}=$ 3300, 3140 (NH_2) and 1690 cm^{-1} (CO); ^{1}H NMR ($CDCl_3$): $\delta=1.31$ (d, 6H, CH_3), 3.22 (m, 1H, CH), 4.74 (br s, 2H, NH_2), 5.09 (s, 2H, CH_2OCONH$_2$), 5.14 (s, 2H, CH_2), 6.65–7.10 (m, 7H, pyridine C3-H and C5-H, pyrrole C2-H and benzene C-H), 8.45–8.48 ppm (m, 2H, pyridine C2-H and C6-H).

5c: 79%; SiO_2 (ethyl acetate); oil; IR: $\tilde{\nu}=3320$, 3120 (NH_2) and 1715 cm^{-1} (CO); ^{1}H NMR (CD_3COCD_3): $\delta=1.29$ (d, 6H, CH_3), 3.18 (m, 1H, CH), 5.07 (s, 2H, CH_2OCONH$_2$), 5.26 (s, 2H, CH_2), 5.95 (br s, 2H, NH_2), 6.42–6.80 (m, 3H, benzene C-H), 6.98–7.04 (m, 2H, pyridine C3-H and C5-H), 7.38 (s, 1H, pyrrole C2-H), 8.42–8.46 ppm (m, 2H, pyridine C2-H and C6-H).

5d: 66%; SiO_2 (ethyl acetate); oil; IR: $\tilde{\nu}=3300$, 3140 (NH_2) and 1700 cm^{-1} (CO); ^{1}H NMR ($CDCl_3$): $\delta=1.30$ (d, 6H, CH_3), 2.24 (s, 3H, $PhCH_3$), 3.27 (m, 1H, CH), 4.80 (br s, 2H, NH_2), 5.08 (s, 2H, CH_2OCONH$_2$), 5.15 (s, 2H, CH_2), 6.53–7.00 (m, 7H, pyridine C3-H and C5-H, pyrrole C2-H and benzene C-H), 8.42–8.46 ppm (m, 2H, pyridine C2-H and C6-H).

5e: 79%; SiO_2 (ethyl acetate); oil; IR: $\tilde{\nu}=3300$, 3140 (NH_2) and 1705 cm^{-1} (CO); ^{1}H NMR ($CDCl_3$): $\delta=1.31$ (d, 6H, CH_3), 2.24 (s, 3H, $PhCH_3$), 3.28 (m, 1H, CH), 4.83 (br s, 2H, NH_2), 5.09 (s, 2H, CH_2OCONH$_2$), 5.14 (s, 2H, CH_2), 6.55–7.10 (m, 7H, pyridine C3-H and C5-H, pyrrole C2-H and benzene C-H), 8.43–8.47 ppm (m, 2H, pyridine C2-H and C6-H).

5f: 65%; SiO_2 (ethyl acetate); 83–85 °C; cyclohexane; IR: $\tilde{\nu}=3310$, 3140 (NH_2) and 1700 cm^{-1} (CO); ^{1}H NMR ($CDCl_3$): $\delta=1.32$ (d, 6H, CH_3), 2.25 (s, 3H, $PhCH_3$), 3.26 (m, 1H, CH), 4.75 (br s, 2H, NH_2), 5.10 (s, 2H, CH_2OCONH$_2$), 5.14 (s, 2H, CH_2), 6.52–7.05 (m, 7H, pyridine C3-H and C5-H, pyrrole C2-H and benzene C-H), 8.43–8.47 ppm (m, 2H, pyridine C2-H and C6-H).

5g: 45%; SiO_2 (ethyl acetate); 112–114 °C; cyclohexane; IR: $\tilde{\nu}=$ 3300, 3140 (NH_2) and 1700 cm^{-1} (CO); ^{1}H NMR ($CDCl_3$): $\delta=1.31$ (d, 6H, CH_3), 2.20 (s, 6H, $PhCH_3$), 3.28 (m, 1H, CH), 4.85 (br s, 2H, NH_2), 5.10 (s, 2H, CH_2OCONH$_2$), 5.14 (s, 2H, CH_2), 6.48 (s, 2H, benzene C2-H and C6-H), 6.70 (s, 1H, benzene C4-H), 6.86–6.90 (m, 2H, pyridine C3-H and C5-H), 7.00 (s, 1H, pyrrole C2-H), 8.43–8.46 ppm (m, 2H, pyridine C2-H and C6-H).

5h: 66%; SiO_2 (ethyl acetate); 112–114 °C; cyclohexane; IR: $\tilde{\nu}=$ 3450, 3340, 3190 (NH_2) and 1695 cm^{-1} (CO); ^{1}H NMR ($CDCl_3$): $\delta=$ 1.28 (d, 6H, CH_3), 3.16 (m, 1H, CH), 3.42 and 4.44 (2br s, 4H, NH_2), 4.93 (s, 2H, CH_2OCONH$_2$), 4.99 (s, 2H, CH_2), 6.64–7.20 ppm (m, 8H, pyrrole C2-H and benzene C-H).

Microbiology: For the antiviral assays, all compounds were solubilized in DMSO at 200 μM and then diluted in culture medium.

Cells and viruses: MT-4 cells were grown at 37 °C in a CO_2 atmosphere (5%) in RPMI 1640 medium, supplemented with fetal calf serum (FCS, 10%), penicillin G (100 IU ml^{-1}), and streptomycin (100 μg mL^{-1}). Cell cultures were checked periodically for the absence of mycoplasma contamination with a MycoTect Kit (Gibco). Human immunodeficiency viruses type-1 (HIV-1, IIIB strain) was obtained from supernatants of persistently infected cells. HIV-1 stock solutions had titers of 1.5×10^7 mL^{-1} for a 50% cell culture infectious dose ($CCID_{50}$).

HIV titration: Titration of HIV was performed in C8166 cells by the standard limiting dilution method (dilution 1:2, four replica wells per dilution) in 96-well plates. The infectious virus titer was determined by light-microscope scoring of syncytia after four days of incubation. Virus titers were expressed as $CCID_{50}$ per mL.

Anti-HIV assays: The activity of the compounds against replication of wild-type HIV-1 in acutely infected cells was based on inhibition of virus-induced cytopathicity in MT-4 cells. Briefly, culture medium (50 μL) containing 1×10^4 cells was added to each well of flat-bottom microtiter trays containing 50 μL culture medium with or without various concentrations of test compounds. Then, 20 μL of HIV suspension (each aliquot containing the appropriate amount of virus (by $CCID_{50}$) to cause complete cytopathicity at day 4) were added. After incubation at 37 °C, cell viability was determined by the 3-(4,5-dimethylthiazol-1-yl)-2,5-diphenyltetrazolium bromide (MTT) method.[28] The cytotoxicity of test compounds was evaluated in parallel with their antiviral activity and was based on the viability of mock-infected cells, as monitored by the MTT method.

RT assays: Assays were performed as previously described.[29] Briefly, purified rRT (20–50 nM) was assayed for its RNA-dependent DNA polymerase activity in a volume of 25 μL containing Tris-HCl (50 mM, pH 7.8), KCl (80 mM), $MgCl_2$ (6 mM), DTT (1 mM), BSA (0.1 mg mL^{-1}), template–primer duplex: [poly(rA)–oligo(dT)$_{12-18}$] (0.3 μM, determined by 3′-OH end concentration), and [^{3}H]dTTP (10 μM, 1 Ci mmole^{-1}). After incubation at 37 °C for 30 min, samples

were spotted onto glass fiber filters (Whatman GF/C) and the acid-insoluble radioactivity was determined.

Computational chemistry: Molecular modeling and graphics manipulations were performed using the SYBYL software package (Sybyl Molecular Modeling System, version 6.9, Tripos Inc., St. Louis, USA) on a Silicon Graphics Tezro workstation equipped with four 700 MHz R16000 processors. Model building of **2**, **4e**, **4j**, **4k**, and **5e** was accomplished with the TRIPOS force field[30] available within SYBYL. Energy minimizations were realized by employing the INSIGHT II/DISCOVER program (Insight II Molecular Modeling Package and Discover 2.2000 Simulation Package, MSI Inc., San Diego, USA), selecting the CVFF force field.[31] Figure 5 was made using PYMOL software.[32]

Docking simulations: Automated docking studies were performed with the docking algorithm GOLD 2.2.[18–22] This automated ligand-docking program uses a genetic algorithm to explore the full range of ligand conformational flexibility with partial flexibility of the receptor. GOLD requires a user-defined binding site. It searches for a cavity within the defined area and considers all the solvent-accessible atoms in the defined area as active-site atoms. On the basis of the GOLD score, for each molecule a bound conformation with high score was considered as the best bound conformation. The score function that was implemented in GOLD consisted basically of H bonding, complex energy, and ligand internal energy terms. A population of possible docked orientations of the ligand is set up at random. Each member of the population is encoded as a "chromosome", which contains information about the mapping of ligand H bond atoms onto (complementary) protein H bond atoms, mapping of hydrophobic points of the ligand onto protein hydrophobic points, and the conformation around flexible ligand bonds and protein OH groups. A number of parameters control the precise operation of the genetic algorithm.

Ligand setup: The core structures of ligands **2**, **4e**, **4j**, **4k**, and **5e** were built using standard bond lengths and bond angles of the SYBYL fragment library. Geometry optimizations were carried out with the SYBYL/MAXIMIN2 minimizer by applying the BFGS (Broyden, Fletcher, Goldfarb, and Shannon) algorithm and setting a rms gradient of the forces acting on each atom of 0.05 kcal mol^{-1} $Å^{-1}$ as the convergence criterion.

Protein setup: The crystal structure of RT–S-1153 (PDB code: 1EPA),[14] recovered from Brookhaven Protein Data Bank was used. The structure was set up for docking as follows: polar and nonpolar hydrogen atoms were added using the BIOPOLYMERS module within SYBYL program (residues Arg, Lys, Glu, and Asp were considered ionized, whereas all His groups were considered neutral by default), and all water molecules were removed.

GOLD docking: An active site of radius 15 Å was defined considering the backbone C=O oxygen atom of Phe 227 as the center of the NNBS. 50 independent docking runs were performed for each docking experiment. All docking runs were carried out using standard default settings with a population size of 100, a maximum number of 100 000 operations, and a mutation and crossover rate of 95. The best generated 10 solutions of each ligand were ranked according to their fitness scores calculated by the GOLD ChemScore function.

To determine whether or not to include the two water molecules found in the RT–S-1153 crystal structure in docking experiments, an active site containing the two water molecules was first defined. The seven highest-scoring solutions found by GOLD were almost identical, and each reproduced the crystallographically determined position and conformation of S-1153 within the NNBS binding site with <0.6 Å rms deviation. To determine the minimum number and combination of water molecules required, water molecules were then systematically removed, giving active sites with combinations of one and zero water molecules in place, and S-1153 was redocked each time. These experiments showed that the position of S-1153 in the active site could be reliably reproduced by docking to a protein with no water molecules in the site.

Energy refinement of the 4k–RT and 5e–RT complexes: To eliminate any residual geometric strain, the obtained complexes were energy minimized using 3000 steps of steepest descent followed by 2000 of conjugate gradient, permitting only the ligand and the protein side chain atoms to relax. The geometry optimization was carried out employing the DISCOVER program with the CVFF force field.

Acknowledgements

The authors thank the Italian Ministero della Sanità—Istituto Superiore di Sanità—V Programma Nazionale di Ricerca sull'AIDS 2003 (grant numbers 30F.19 and 40F.78), and Italian MIUR (PRIN 2004) for financial support.

Keywords: AIDS · antiviral agents · arylthiopyrroles · HIV · NNRTI

[1] F. J. Palella, K. M. Delaney, A. C. Moorman, M. O. Loveless, J. Fuhrer, G. A. Satten, D. J. Aschman, S. D. Holmberg, *N. Engl. J. Med.* **1998**, *338*, 853–860.
[2] S. Vella, L. Palmisano, *Antiviral Res.* **2000**, *45*, 1–7.
[3] G. Hajos, Z. Riedl, J. Molnar, D. Szabo, *Drugs Future* **2000**, *25*, 47–62.
[4] W. Schäfer, W.-G. Friebe, H. Leinert, A. Mertens, T. Poll, W. von der Saal, H. Zilch, B. Nuber, M. L. Ziegler, *J. Med. Chem.* **1993**, *36*, 726–732.
[5] L. A. Kohlstaedt, J. Wang, J. M. Friedman, P. A. Rice, T. A. Steitz, *Science* **1992**, *256*, 1783–1790.
[6] "Reservoirs for HIV-1": R. F. Siliciano, *Curr. Infect. Dis. Rep.* **1999**, *1*, 298–304.
[7] M. R. Furtado, D. S. Callaway, J. P. Phair, K. J. Kunstman, J. L. Stanton, C. A. Macken, A. S. Perelson, S. M. Wolinsky, *N. Engl. J. Med.* **1999**, *340*, 1614–1622.
[8] R. A. Koup, V. J. Merluzzi, K. D. Hargrave, J. Adams, K. Grozinger, R. J. Eckner, J. L. Sullivan, *J. Infect. Dis.* **1991**, *163*, 966–970.
[9] W. W. Freimuth, *Adv. Exp. Med. Biol.* **1996**, *394*, 279–289.
[10] S. D. Young, S. F. Britcher, L. O. Tran, L. S. Payne, W. C. Lumma, T. A. Lyle, J. R. Huff, P. S. Anderson, D. B. Olsen, S. S. Carroll, D. J. Pettibone, J. A. O'Brien, R. G. Ball, S. K. Balani, J. H. Lin, I.-W. Chen, W. A. Schleif, V. V. Sardana, W. J. Long, V. W. Byrnes, E. A. Emini, *Antimicrob. Agents Chemother.* **1995**, *39*, 2602–2605.
[11] E. De Clercq, *Chem. Biodiversity* **2004**, *1*, 44–64.
[12] D. C. Meadows, J. Gervay-Hague, *ChemMedChem* **2006**, *1*, 16–29.
[13] a) T. Fujiwara, A. Sato, M. El-Farrash, S. Miki, K. Abe, Y. Isaka, M. Kodama, Y. Wu, L. B. Chen, H. Harada, H.; Sugimoto, M. Hatanaka, Y. Hinuma, *Antimicrob. Agents Chemother.* **1998**, *42*, 1340–1345; b) T. Fujiwara, A. Sato, A. K. Patick, K. E. Potts, *Int. Antiviral News* **1999**, *7*, 18–20.
[14] J. Ren, C. Nichols, L. E. Bird, T. Fujiwara, H. Sugimoto, D. I. Stuart, D. K. Stammers, *J. Biol. Chem.* **2000**, *275*, 14316–14320.
[15] M. Hajima, Y. Hozumi, M. Kabaki, WO 199829395, **1998** [*Chem. Abstr.* **1998**, *129*, 95494].
[16] R. Di Santo, R. Costi, M. Artico, R. Ragno, S. Massa, M. La Colla, R. Loddo, P. La Colla, A. Pani, *Med. Chem. Res.* **2002**, *12*, 153–167.
[17] V. J. Merluzzi, K. D. Hargrave, M. Labadia, K. Grozinger, M. Skoog, J. C. Wu, C.-K. Shih, K. Eckner, S. Hattox, J. Adams, A. S. Rosenthal, R. Faanes, R. J. Eckner, R. A. Koup, J. L. Sullivan, *Science* **1990**, *250*, 1411–1413.
[18] GOLD 2.2, CCDC Software Limited, Cambridge, UK, **2004**.

[19] G. Jones, P. Willett, R. C. Glen, A. R. Leach, R. J. Taylor, *J. Mol. Biol.* **1997**, *267*, 727 – 748.
[20] G. Jones, P. Willett, R. C. Glen, *J. Mol. Biol.* **1995**, *245*, 43 – 53.
[21] C. Bissantz, G. Folkers, D. Rognan, *J. Med. Chem.* **2000**, *43*, 4759 – 4767.
[22] G. Schneider, H. Bohm, *Drug Discovery Today* **2002**, *7*, 64 – 70.
[23] R. F. Schinazi, B. A. Larder, J. W. Mellors, *Int. Antiviral News* **1997**, *5*, 129 – 135.
[24] R. Esnouf, J. Ren, C. Ross, Y. Jones, D. Stammers, D. Stuart, *Nat. Struct. Biol.* **1995**, *2*, 303 – 308.
[25] Y. Hsiou, J. Ding, K. Das, A. D. Clark, Jr., P. L. Boyer, P. Lewi, P. A. J. Janssen, J. P. Kleim, M. Rösner, S. H. Hughes, E. Arnold, *J. Mol. Biol.* **2001**, *309*, 437 – 445.
[26] F. Rodriguez-Barrios, J. Balzarini, F. Gago, *J. Am. Chem. Soc.* **2005**, *127*, 7570 – 7578.
[27] A. Lavecchia, R. Costi, M. Artico, G. Miele, E. Novellino, A. Bergamini, E. Crespan, G. Maga, R. Di Santo, *ChemMedChem* **2006**, *1*, 1379 – 1390.
[28] R. Pauwels, J. Balzarini, M. Baba, R. Snoeck, D. Schols, P. Herdewijn, J. Desmyter, E. De Clercq, *J. Virol. Methods* **1988**, *20*, 309 – 321.
[29] M. Botta, M. Artico, S. Massa, A. Gambacorta, M. E. Marongiu, A. Pani, P. La Colla, *Eur. J. Med. Chem.* **1992**, *27*, 251 – 257.
[30] J. G. Vinter, A. Davis, M. R. Saunders, *J. Comput.-Aided Mol. Des.* **1987**, *1*, 31 – 51.
[31] A. T. Hagler, S. Lifson, P. Dauber, *J. Am. Chem. Soc.* **1979**, *101*, 5122 – 5130.
[32] "The PyMOL Molecular Graphics System": W. L. DeLano, **2002** http://pymol.sourceforge.net/.

Received: May 16, 2006
Revised: August 9, 2006
Published online on November 7, 2006

